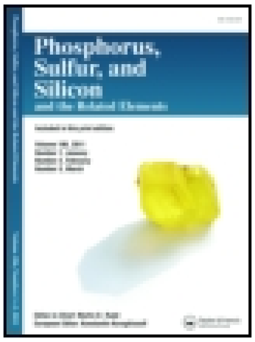

Phosphorus, Sulfur, and Silicon and the Related Elements

ISSN: (Print) (Online) Journal homepage: https://www.tandfonline.com/loi/gpss20

Synthesis, characterization, and *in vitro* anticancer studies of chlorido(triphenylphosphine)ruthenium(II) dithiocarbamate complexes

Peter A. Ajibade & Fartisincha P. Andrew

PHOSPHORUS, SULFUR, AND SILICON AND THE RELATED ELEMENTS
https://doi.org/10.1080/10426507.2021.1925671

Taylor & Francis
Taylor & Francis Group

Synthesis, characterization, and *in vitro* anticancer studies of chlorido(triphenylphosphine)ruthenium(II) dithiocarbamate complexes

Peter A. Ajibade and Fartisincha P. Andrew

School of Chemistry and Physics, University of KwaZulu-Natal, Scottsville, Pietermaritzburg, South Africa

ABSTRACT

Three chlorido(triphenylphosphine)ruthenium(II) dithiocarbamate complexes - $[RuCl(PPh_3)_3(Mbzdtc)]$ **1**, $[RuCl(PPh_3)_3(Ppipdtc)]$ **2**, and $[RuCl(Ph_3)_3(Mordtc)]$ **3** with Mbzdtc = *N*-methylphenyldithiocarbamate, Ppipdtc = phenylpiperazyldithiocarbamate and (Mordtc) = morpholinyldithiocarbamate were synthesized and characterized by elemental analysis and spectroscopic techniques. The Ru(II) atom is six coordinate and displays an octahedral coordination geometry, in which it is bonded to one dithiocarbamato anion acting as bidentate ligand. Electrochemical studies indicate for complexes **1** and **2** a quasi-reversible one electron redox couple due to Ru(III)/Ru(II), whereas complex **3** showed two redox couples due to Ru(III)/Ru(II) and Ru(II)/Ru(I). The $E_{1/2}$ values observed toward the cathodic region are consequence of the presence of S-S donor atom of the dithiocarbamate ligand. The anticancer potential of the complexes was assessed using sulforhodamine B (SRB) assay against renal (TK10) melanoma (UACC62) and breast (MCF7) human cancer cell lines. Complex **1** exhibits the highest cytotoxic activity against MCF7 with an IC_{50} value of 33.36 μM, whereas complex **3** exhibits the lowest activity against TK10 with an IC_{50} value of 91.95 μM.

ARTICLE HISTORY
Received 23 October 2020
Accepted 29 April 2021

KEYWORDS
Ruthenium(II); dithiocarbamate; triphenylphosphine; anticancer; electrochemical study

GRAPHICAL ABSTRACT

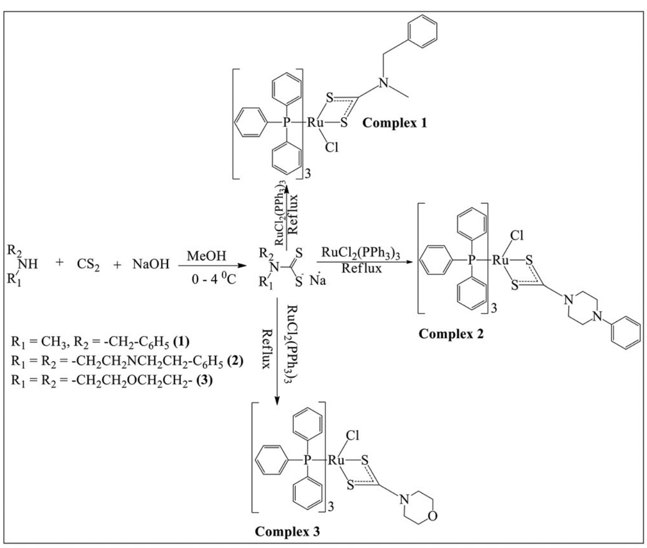

Introduction

The introduction of cisplatin in 1965 as anticancer agent has been a great breakthrough in the development of metallo-pharmaceuticals.[1] This led to the discovery of many other platinum-based drugs such as nedaplatin, carboplatin, oxaliplatin, heptaplatin, and laboplatin. Although cisplatin and analogues are the best metallo-based therapeutic agents that are used in about 70% of the cancer cases[2] they are often constrained by severe toxicity, resistance, and narrow activity range.[3] Their nonspecific target of DNA and reaction with proteins such as metallothioneins, thioredoxine, and other thiol-containing molecules like cysteine, reduced glutathione and methionine provide a pathomechanism of the various side effects associated with their clinical application.[4] Consequently, there has been a consistent search for new compounds of other transition metals other than the

CONTACT Peter A. Ajibade ajibadep@ukzn.ac.za School of Chemistry and Physics, University of KwaZulu-Natal, Scottsville, Pietermaritzburg, South Africa.
Supplemental data for this article is available online at https://doi.org/10.1080/10426507.2021.1925671.

Table 1. Electronic spectra of ligands and complexes.

Compounds	Wavelength (λ_{max} nm)	Assignment
Mbzdtc, L_1	258, 285 (shoulder)	n-π*/π-π* intraligand
Mbzdtc, L_2	261, 286 (shoulder)	n-π*/π-π* intraligand
Mordtc, L_3	261, 287(shoulder)	n-π*/π-π* intraligand
[RuCl(PPh$_3$)$_3$(Mbzdtc)] **(1)**	229	n-π*/π-π* intraligand
	267–546	MLCT
[RuCl(PPh$_3$)$_3$(Ppipdtc)] **(2)**	230, 259	n-π*/π-π* intraligand
	322–418	MLCT
[RuCl(PPh$_3$)$_3$(Mordtc)] **(3)**	229, 264	n-π*/π-π* intraligand
	321–429	MLCT

Table 2. Summary of electrochemical data (V) recorded in CH_2Cl_2 at 25 mVs^{-1}using $TBAPF_6$ supporting electrolyte $\Delta E_p = E_{pa} - E_{pc}$, $E_{1/2} = (E_{pa} - E_{pc})/2$.

Complexes	E_{pc} (V)	E_{pa} (V)	ΔE_p (V)	$E_{1/2}$ (V)	Range of scan
[RuCl(PPh$_3$)$_3$(Mbzdtc)] **(1)**	−0.0389	0.1877	0.23	0.0744	−0.21 to 0.39 V
[RuCl(PPh$_3$)$_3$(Ppipdtc)] **(2)**	0.7049	1.0373	0.33	0.8711	0 to 1.4 V
[RuCl(PPh$_3$)$_3$(Mordtc)] **(3)**	1.0228	1.2091	0.19	1.1160	−0.12 to 1.28 V
	0.0912	0.3581	0.27	0.2247	

classical platinum-based anticancer agents with the aim of overcoming the side effect associated with the platinum-based compounds.

In recent years, ruthenium-based complexes are being studied as viable alternative to platinum-based anticancer agents, which has led to the discovery of the therapeutic potentials of *trans*-[Ru(Im)(DMSO)Cl$_4$](Him) (NAMI-A) and *trans*-[Ru(Ind)$_2$Cl$_4$](Hind) KP1019 (Ind = imidazole).[5] Although the mechanisms of action of these ruthenium compounds are still a matter of debate, ruthenium(II) and ruthenium(III) oxidation states are known to be stable at physiological conditions and are generally regarded as redox-activatable prodrugs.[6–8] NAMI-A and KP1019 belong to this class of compounds and could be activated *in vivo* via the reduction of ruthenium(III) to more active ruthenium(II) species in the low oxygen environment of the solid tumors.[9–12] Ruthenium belongs to the same triad as iron and could mimic iron in binding to biomolecules, as it can easily bind proteins such as transferrin (known to transport iron in the body).[13] Cancer cells possess more transferrin receptors than normal cells,[14] although it is argued that binding to transferrin does not necessarily mean tumor cell accumulation. Tumor cells are believed to require more iron than the healthier cells because they have more faster cyclic activity compared to their healthier cell counterparts, hence, they express large amount of transferrin receptors to get this essential element. This means tumor cell accumulation by transferrin might influence the ability of ruthenium compounds to bind to DNA or other biomolecules.[15]

The development of metal-based therapeutic agents has shown that *in vitro* and *in vivo* activities of metal complexes can be fine-tuned by subtle changes in the coordinated ligands. Many ruthenium complexes with ligands such as azo-quinolines, polypyridyl, Schiff bases, thiosemicarbazones, arenes, and dithiocarbamate, have been reported for their cytotoxic activity.[16–21] However, very little has been done on ruthenium(II) dithiocarbamate complexes as anticancer agents.[22,23] Therefore, in view of this and the growing concern in the design of metal complexes as anticancer agents, we report the synthesis, characterization, electrochemistry, and *in vitro* anticancer screening of chlorido(triphenylphosphine) ruthenium(II) dithiocarbamate complexes. The choice of the dithiocarbamate ligand lies in their ability to stabilize wide range of metal ions at different oxidation states coupled with their rich electrochemistry and excellent biological activity.[24,25] The complexes were screened against renal (TK10) melanoma (UACC62) and breast (MCF7) human cancer cell lines to evaluate their anticancer potential.

Results and discussion

Synthesis and physicochemical data

The complexes [RuCl(PPh$_3$)$_3$(Mbzdtc)], [RuCl(PPh$_3$)$_3$ (Ppipdtc)], and [RuCl(PPh$_3$)$_3$(Mordtc)] were synthesized by the reaction of chloridotris(triphenylphosphine)ruthenium(II) and *N*-methylbenzyl-, phenylpiperazyl-, and morpholinyl-dithiocarbamate ligands in 1:1 ratio as presented in Scheme 1.

All the complexes were isolated as air stable solids in moderate yields with melting points ranging from 189 to 217 °C. The complexes were highly soluble in dichloromethane, chloroform and DMSO but insoluble in toluene, hexane, and benzene. The molar conductance of the complexes in the range of 2.94 – 12.50 Ohm^{-1}cm^{2}mol^{-1} measured in DMSO indicated that the complexes are non-electrolytes in solution.

FTIR spectroscopic studies

The FTIR spectra of the ligands and complexes due to ν(C—N) and ν(C—S) stretching vibrations were compared to deduce the mode of coordination of the ligands to the ruthenium(II) ion. A single sharp ν(C—N) vibrational band was observed at 1498 cm^{-1} and 1492 cm^{-1} for complexes **1** and **2**, respectively, as compared to those of the corresponding free ligands, L_1 (1625 cm^{-1}) and L_2 (1494 cm^{-1}). In complex **3**, however, the vibrational frequency is observed at 1467 cm^{-1} compared to the free ligand at 1418 cm^{-1}. Other studies have shown that single sharp bands in the range of 1450–1550 cm^{-1} in dithiocarbamate complexes are typical of carbon nitrogen bond order that is intermediate between the stretching frequencies associated with C—N single bond (1250–1350 cm^{-1}) and double bond (1640–1690 cm^{-1}).[26,27] The shift observed in the metal complexes relative to those of the free ligands is consistent with an increase in double bond character of the C—N bon as a consequence of the delocalization of electrons within the dithiocarbamate anion bonded to the Ru(II) ion. In addition, the presence of a single sharp ν(C—S) band in the region of 1021–1026 cm^{-1} indicates a symmetrical coordination of the dithiocarbamate anions to the Ru(II) ion. This confirmed that the dithiocarbamate anion acts as a bidentate chelating ligand to the Ru(II) ion, otherwise two bands at approximately 1000 ± 70 cm^{-1} would have been observed for monodentately coordinated dithiocarbamate anion.[26–37]

Table 3. IC_{50} (μM) values of the Ru(II) complexes tested against renal (TK10), UACC62 (melanoma), and breast (MCF7) cancer lines.

Complexes	TK10 (μM)	UACC62 (μM)	MCF7 (μM)
[RuCl(PPh_3)$_3$(Mbzdtc)] **(1)**	79.39	39.28	33.36
[RuCl(PPh_3)$_3$(Ppipdtc)] **(2)**	77.18	72.32	38.18
[RuCl(PPh_3)$_3$(Mordtc)] **(3)**	91.95	90.20	41.07
Parthenolide	4.64	11.37	3.52

Electronic spectra

The electronic spectra of the ligands and the corresponding Ru(II) complexes are shown in Supporting Information Figures S5, S10 and S15 for complexes **1**, **2**, and **3**, respectively, and relevant data are presented in Table 1. The spectra are dominated by ligands to metal charge transfer electronic transitions.

An electronic transition in the range of 258–261 nm with a shoulder at 285–286 nm observed in the free ligands was assigned to n-π^*/π-π^* intraligand transitions. These absorptions shifted in all complexes with the appearance of shoulders. A broad absorption band in the range of 267–546 nm for complex **1**, 322–418 nm for complex **2**, and 321–429 nm for complex **3** is assigned to metal to ligand charge transfer transitions.[38]

^{1}H and ^{31}P NMR spectra

The ^{1}H NMR spectra of the complexes **1 – 3** showed multiplets in the range 7.70–7.05 ppm (Supporting Information Figures S16, S17 and S18, respectively). These multiplets are due to the triphenylphosphine co-ligand and appeared a little upfield relative to the aromatic signals of the free dithiocarbamate ligands. The ^{31}P NMR spectra showed a single peak at 29.0 and 25.5 ppm for complexes **1** and **2**, respectively, which indicate that the phosphorus atoms of the triphenylphosphine co-ligands are magnetically equivalent in these complexes. However, complex **3** showed two peaks at 29.0 and 53.0 suggesting that the phosphorus atoms of the phosphines are magnetically nonequivalent.[39]

Electrochemistry

The redox properties of the three complexes were probed using cyclic voltammetry and square wave at a scan rate of 25 mV/s. The electrochemical data is presented in Table 2. The voltammogram of complex **1** (Supporting Information Figure S19) displays a cathodic peak potential of E_{pc} = −0.0389 V and a corresponding anodic peak potential of E_{pa} = 0.1877 V in the range −0.21 − 0.39 V. The peak separation (ΔE_p) is 0.23 V and $E_{1/2}$ = 0.0744 V. The increase in the value of ΔE_p with increasing scan rate provides evidence for quasi-reversible Ru III/II couple.[40,41] Similarly, complex **2** (Supporting Information Figure S20) was studied at 0 − 1.4 V potential range. The cathodic peak potential is E_{pc} = 0.7049 V and the corresponding anodic peak potential is E_{pa} = 1.0373 V. The ΔE_p value is 0.33 V and $E_{1/2}$ = 0.8711 V, the increase of ΔE_p with increasing scan rate indicates a quasi-reversible one electron process due to Ru III/II. The square wave (Supporting Information Figure S21) also confirms this redox process. However, complex **3** exhibits two quasi reversible redox peaks (Supporting Information Figure S22): the first at E_{pc} = 1.0228 V and the corresponding oxidation peak at E_{pa} = 1.2091 V with ΔE_p = 0.19 V and the second at E_{pc} = 0.0912 V and the oxidation peak at E_{pa} = 0.3581 V with peak separation ΔE_p = 0.27 V. This is also confirmed in the square wave scan (Supporting Information Figure S23) where two peaks at the same region were observed. The first peak may be attributed to Ru(III)/Ru(II) couple and the second may be due to Ru(II)/Ru(I) couple. The $E_{1/2}$ values observed toward the cathodic region in the voltammogram are a consequence of the presence of S-S donor group of the dithiocarbamate ligands. This is consistent with the proposition by Devagi et al. that hard donor atoms tend to give more negative $E_{1/2}$ values whereas soft donor atoms such as dithiocarbamate give positive $E_{1/2}$ values.[42,43]

Anticancer studies

The complexes were screened using sulforhodamine B (SRB) assay for their anticancer activity against renal (TK10), UACC62 (melanoma), and breast (MCF7) human cancer cell lines. The half maximum inhibitory concentrations (IC_{50}) that inhibit growth of the cancer cells are presented in Table 3. The complexes exhibit low to moderate cytotoxicity against the three cancer cell lines with IC_{50} values ranging from 33.36 to 91.95 μM. The anticancer potency of the cell lines. The activity of the compounds is relatively lower compared to that reported for Cu(II) and Zn(II) complexes against these cancer cell lines.[25,44–46] Complexes **1**, **2**, and **3** were moderately active against MCF7 with IC_{50} values of 33.36, 38.18, and 41.07 μM, respectively. Complex **1** also exhibits a good activity against UACC62 cell line with IC_{50} value of 39.28. However, the activity of all complexes was comparatively low against TK10 cell line with IC_{50} between 77.18 and 91.95 μM. Similarly, the activity of complexes **2** and **3** were relatively low against UACC62 with IC_{50} 72.32 and 90.20 μM, respectively. Although one cannot ascertain the reason for the relative activity of the three compounds against MCF7, the ruthenium(II) complexes have a capacity to reduce the energy status in tumors as well as to enhance tumor hypoxia, which also influences their antitumor activities.[47] Similarly, mixed ligand complexes tend to have enhanced biological activity.[48]

Experimental

Materials and methods

All starting materials were purchased from Aldrich and used without further purification. The ^{1}H NMR spectra were recorded at 400 MHz and the ^{13}C NMR spectra at 100 MHz with a Bruker Avance III 400 MHz spectrometer at room temperature using TMS as internal reference. All the proton and carbon NMR shifts are quoted in ppm and relative to relevant solvent signal. FTIR spectra were recorded in the region 4000–500 cm^{-1} using Perkin Elmer spectrum 100 FTIR spectrometer. The UV–Visible spectra were recorded using Cary100-UV–Vis spectrophotometer. Molar conductivity was measured with Jenway 4510 conductivity meter using 10^{-3} $molL^{-1}$ freshly prepared solutions of the compounds. Human cancer cell lines TK10 (renal), UACC62 (melanoma), and MCF7 (breast) were obtained from National Cancer Institute (NCI) in the framework a collaborative research program between the Council for Scientific and Industrial Research (CSIR), South Africa, and NCI. *In vitro* cytotoxic activity of the compounds was tested using sulforhodamine B (SRB) assay. Electrochemical measurements for the ruthenium complexes were performed with Autolab potentiostat (with Nova 1.7 software) equipped with three electrode system; a glassy carbon working electrode (GCWE), Ag/AgCl reference electrode and an auxiliary platinum counter electrode. Fresh 2 mM solution of the complexes and the supporting electrolyte (0.1 M tetrabutylammonium hexafluorophosphate) was prepared in dichloromethane. All solutions were purged with nitrogen steam for about 10 min before every experiment. The glassy carbon working electrode is polished between each run with slurry of alumina and ultra-pure water on Buehler felt pad and rinsed thoroughly with ultra-pure water.

Synthesis of sodium N-methylbenzyldithiocarbamate (Mbzdtc)

A method reported in the literature[44] was adopted for the synthesis of this ligand. NaOH (2.0 g, 50 mmol) was added to methanolic solution of *N*-methylbenzylamine (6.0 g, 50 mmol) and stirred for 30 min, followed by the addition of cold carbon disulfide (3.8 g, 50 mmol). The reaction mixture was stirred for 4 h at 0–4 °C; the resulting white precipitate was filtered, washed several times with diethyl ether, and dried under vacuum over silica. Yield, 96%, m.p 129 °C, Λ_m(Ohm^{-1} cm^2 mol^{-1}): 44.60, Anal. Calcd for $Na(S_2CNCH_3CH_2C_6H_5) \cdot 2H_2O$: C, 42.34; H, 5.53; N, 5.49; S, 25.12. Found: C, 42.20; H, 5.60; N, 5.46; S, 25.54%. ^1H NMR (400 MHz, D_2O) $\delta = 7.52$ (t, $^3J_{HH}$ = 8.0 Hz, 2H, $C_6\boldsymbol{H}_5$,), 7.42 (t, $^3J_{HH}$ = 8.0 Hz, 1H, $C_6\boldsymbol{H}_5$,), 7.36 (d, $^3J_{HH}$ = 4.0 Hz, 2H, $C_6\boldsymbol{H}_5$), 5.50 (s, 2H), 3.50 (s, 3H). ^{13}C NMR (400 MHz, D_2O): $\delta = 210.1$ (CS), 42.7 (N-CH_3), 59.6 (N-CH_2-(C_6H_5)), 136.8, 126.8, 127.4, 128.9 (-C_6H_5), UV–Vis (H_2O): λ_{max} = 258, 285 nm. Selected IR data (solid state): 1625, $\nu_{(C\text{-}N)}$; 949, $\nu_{(C\text{-}S)}$ cm^{-1}.

Synthesis of sodium phenylpiperazyldithiocarbamate (Ppipdtc)

The ligand was prepared according to literature.[45] Two millilitre of a cold aqueous solution of NaOH (2.0 g, 50 mmol) was added to 15 mL of a cold methanolic solution of 1-phenylpiperazine (8.07 g, 50 mmol) followed by the addition of cold carbon disulfide (3.80 g, 50 mmol). The reaction mixture was stirred for 4 h at 0–4 °C; the resulting white precipitate formed was filtered, washed several times with diethyl ether and dried over silica. Yield 78%, m.p 159 °C, Λ_m (Ohm^{-1} cm^2 mol^{-1}): 67.52, white solid, Anal. Calcd for $Na(S_2CNC_4H_8NC_6H_5) \cdot 2H_2O$: C, 44.58; H, 5.78; N, 9.45; S, 21.64. Found: C, 44.28; H, 5.82; N, 9.35; S, 21.92%. ^1H NMR (400 MHz, D_2O): $\delta = 7.41$ (t, $^3J_{HH}$ = 8.0 Hz, 2H, $C_6\boldsymbol{H}_5$,), 7.17 (d, $^3J_{HH}$ = 8.0 Hz, 2H, $C_6\boldsymbol{H}_5$,), 7.08 (t, $^3J_{HH}$ = 8.0 Hz, 1H, $C_6\boldsymbol{H}_5$,), 4.50 (t, $^3J_{HH}$ = 8.0 Hz, 4H, $C\boldsymbol{H}_2$,), 3.24 (t, $^3J_{HH}$ = 4.0 Hz, 4H, $C\boldsymbol{H}_2$,). ^{13}C NMR (400 MHz, D_2O): $\delta = 209.0$ (CS), 49.7, 50.5 (N-CH_4CH_4N-), 118.0, 122.2, 129.6, 150.3 (-C_6H_5). UV–Vis (H_2O): λ_{max} = 261, 286 nm (shoulder). Selected IR data (solid state): 1494, $\nu_{(C\text{-}N)}$; 994, $\nu_{(C\text{-}S)}$ cm^{-1}.

Synthesis of sodium morpholinyldithiocarbamate (Mordtc)

The sodium salt of morpholinedithiocarbamate was prepared according to literature procedure.[40,42,43] To equimolar amounts of morpholine (4.44 g, 50 mmol) dissolved in 20 mL of methanol and NaOH (2.0 g, 50 mmol) cold carbon disulfide (3.80 g, 50 mmol) was added. The reaction mixture was stirred for 4 h at 0–4 °C; the resulting white precipitate was filtered, washed several times with diethyl ether, and dried under vacuum over silica. Yield 65%, m.p 185 °C, Λ_m (Ohm^{-1} cm^2 mol^{-1}): 66.30. Anal. Calcd for $Na(S_2CNC_4H_8O) \cdot H_2O$: C, 29.55; H, 4.96; N, 6.89; S, 31.55. Found: C, 29.18; H, 5.04; N, 6.92; S, 32.08%. ^1H NMR (400 MHz, D_2O): $\delta = 4.45$ (t, $^3J_{HH}$ = 8.0 Hz, 4H, $C\boldsymbol{H}_2$,), 3.84 (t, $^3J_{HH}$ = 8.0 Hz, 4H, $C\boldsymbol{H}_2$). ^{13}C NMR (400 MHz, D_2O): $\delta = 209.4$ (CS), 51.4, 66.1 (OCH_4CH_4N-). UV–Vis (H_2O): λ_{max} = 264, 286(shoulder) nm. Selected IR data (solid state): 1418, $\nu_{(C\text{-}N)}$; 979, $\nu_{(C\text{-}S)}$ cm^{-1}.

Synthesis of [RuCl(PPh3)3(Mbzdtc)] 1

N-Methylbenzyldithiocarbamate (0.0228 g, 0.104 mmol) and $[RuCl_2(PPh_3)_3]$ (0.10 g, 0.104 mmol) were refluxed in 20 mL of methanol for 4 h. The resulting greenish like solution was allowed to cool to ambient temperature. The precipitate formed was filtered and washed with diethyl ether. Yield 58%, green solid, m.p 203 °C, Anal. Calcd for $[Ru(S_2CNCH_3CH_2C_6H_5Cl(PPh_3)_3] \cdot 4.5H_2O$: C, 62.70; H, 5.35; N, 1.18; S, 5.40. Found: C, 62.67; H, 5.19; N, 1.72; S, 5.09%. Λ_m (Ohm^{-1} cm^2 mol^{-1}): 12.50. ^1H NMR (400 MHz, $CDCl_3$): $\delta = 7.70$-7.43 (m, 50H), 5.98 (s, 2H), 3.79 (s, 3H). ^{31}P NMR (400 MHz, $CDCl_3$): $\delta = 29.0$. Selected IR data (solid state): 1498, $\nu_{(C\text{-}N)}$; 1024, $\nu_{(C\text{-}S)}$ cm^{-1}. UV–Vis (CH_2Cl_2): λ_{max} = 229, 267–546 nm.

Synthesis of [RuCl(PPh3)3(Ppipdtc)] 2

Phenylpiperazyldithiocarbamate (0.104 mmol, 0.0270 g) and $[RuCl_2(PPh_3)_3]$ (0.104 mmol, 0.10 g) were refluxed in 20 mL methanol for 4 h, the resulting greenish like solution was allowed to cool. The precipitate formed was filtered and washed with diethyl ether. Yield 52%, green solid, m.p 189 °C, Λ_m (Ohm^{-1} cm^2 mol^{-1}): 11.11. Anal. Calcd for $[Ru(S_2CNC_4H_8NC_6H_5)Cl(PPh_3)_3] \cdot 2H_2O$: C, 65.23; H, 5.22; N, 2.34; S, 5.36. Found: C, 65.55; H, 4.95; N, 2.01; S, 5.79%. ^1H NMR (400 MHz, $CDCl_3$): $\delta = 7.79$-7.06 (m, 50H), 5.94 (s, 4H), 3.50 (s, 4H). ^{31}P NMR (400 MHz, $CDCl_3$): $\delta = 29.0$, Selected IR data (solid state): 1492, $\nu_{(C\text{-}N)}$; 1026, $\nu_{(C\text{-}S)}$ cm^{-1}. UV–Vis (CH_2Cl_2): λ_{max} = 230, 259, 322–418 nm.

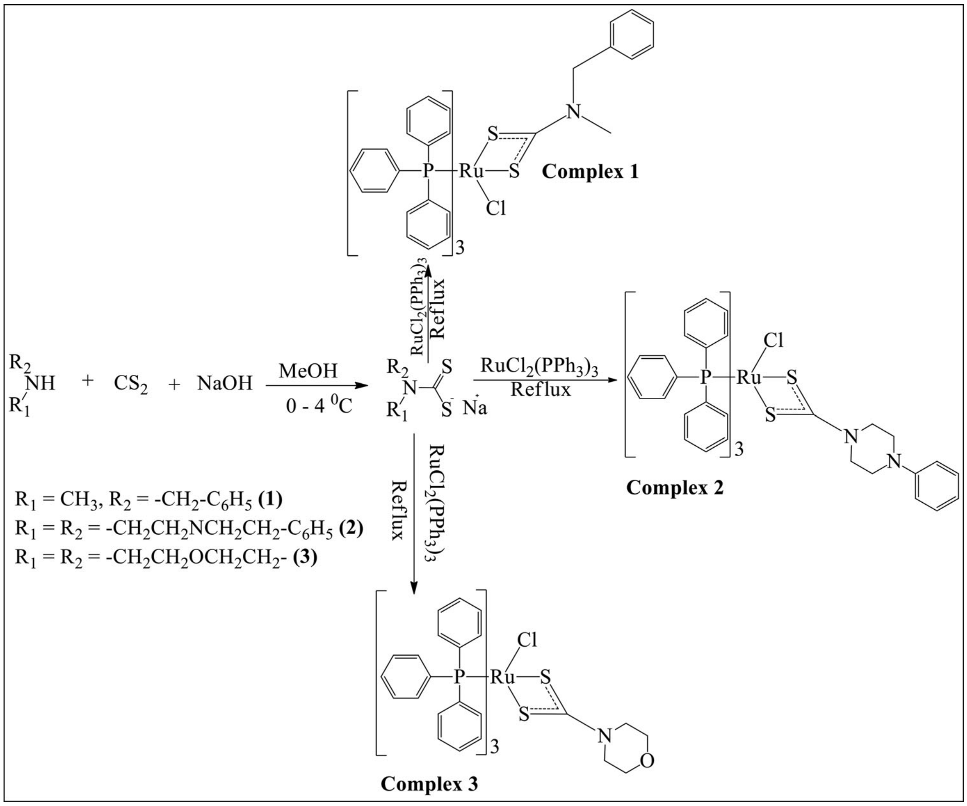

Scheme 1. Synthesis of complexes **1–3**.

Synthesis of [RuCl(Ph$_3$)$_3$(Mordtc)] 3

Morpholinyldithiocarbamate (0.104 mmol, 0.0193 g) and [RuCl$_2$(PPh$_3$)$_3$] (0.104 mmol, 0.10 g) were refluxed in 20 mL of methanol for 4 h. The resulting greenish like solution was allowed to cool to ambient temperature. The precipitate formed was filtered and washed with diethyl ether. Yield 58%, m.p. 217 °C, green solid, Λ_m (Ohm^{-1} cm^2 mol^{-1}): 2.94. Anal. Calcd for [Ru(S$_2$CNC$_4$H$_8$OCl(PPh$_3$)$_3$] · 2 H$_2$O: C, 63.06; H, 4.74; N, 1.27; S, 5.81. Found: C, 63.01; H, 4.87; N, 0.82; S, 5.99%. ^{1}H NMR (400 MHz, CDCl$_3$): $\delta = 7.70$-7.06 (m, 45H), 5.95 (s, 4H), 3.50 (s, 4H). ^{31}P NMR (400 MHz, CDCl$_3$): $\delta = 29.0$. Selected IR data (solid state): 1467, $\nu_{(C\text{-}N)}$; 1021, $\nu_{(C\text{-}S)}$ cm^{-1}. UV–Vis (CH$_2$Cl$_2$): λ_{max} = 229, 264, 321-429 nm.

Conclusion

Three chlorido(triphenylphosphine)ruthenium(II) dithiocarbamate complexes - [RuCl(PPh$_3$)$_3$(Mbzdtc)], [RuCl(PPh$_3$)$_3$ (Ppipdtc)], and [RuCl(PPh$_3$)$_3$(Mordtc)] – were synthesized and characterized by FTIR, UV–Vis, and NMR spectroscopy, elemental analysis, and cyclic voltammetry. The elemental and spectroscopic data agree with the proposed composition and structure of the compounds. The electrochemical studies showed one reversible Ru(III)/Ru(II) redox couple in the voltammogram of complexes **1** and **2**, whereas for complex **3** two redox couples due to Ru(III)/Ru(II) and Ru(II)/Ru(I) were observed, which was further confirmed by their square wave plots. The *in vitro* anticancer activity of the Ru(II) complexes was evaluated against three human cancer cell lines: renal (TK10), melanoma (UACC62), and breast (MCF7) using sulforhodamine B (SRB) assay. Complex **1** with methyl benzyldithiocarbamate is the most active followed by complex **2** with phenylpiperazyldithiocarbamate while complex **3** with morpholinyldithiocarbamate showed low anticancer activity. The results indicate that coordination of different dithiocarbamate anions with to chlorido(triphenylphosphine) ruthenium(II) result in different cytotoxic activities against the cancer cell lines. The design of the complexes can be modified to obtain more potent compounds.

Disclosure statement

No potential conflict of interest was reported by the authors.

Funding

The authors acknowledge the financial support of Sasol and of National Research Foundation, South Africa.

References

[1] Vajs, J.; Steiner, I.; Brozovic, A.; Pevec, A.; Ambriović-Ristov, A.; Matković, M.; Piantanida, I.; Urankar, D.; Osmark, M.; Košmrlj, J. The 1,3-Diaryltriazenido(p-Cymene)Ruthenium(II) Complexes with a High In Vitro Anticancer Activity. *J. Inorg. Biochem.* **2015**, *153*, 42–48. DOI: 10.1016/j.jinorgbio.2015.09.005.

[2] Adeniyi, A. A.; Ajibade, P. A. Computational Properties of η6-Toluene and η6-Trifluorotoluene Half-Sandwich Ru(II) Anticancer Complexes. *J. Biomol. Struct. Dyn.* **2014**, *32*, 1351–1365. DOI: 10.1080/07391102.2013.819299.

[3] McWhinney, S. R.; Goldberg, R. M.; McLeod, H. L. Platinum Neurotoxicity Pharmacogenetics. *Mol. Cancer Ther.* **2009**, *8*, 10–16. DOI: 10.1158/1535-7163.MCT-08-0840.

[4] Shahsavani, M. B.; Ahmadi, S.; Aseman, M. D.; Nabavizadeh, S. M.; Rashidi, M.; Asadi, Z.; Erfani, N.; Ghasemi, A.; Saboury, A. A.; Niazi, A.; et al. Anticancer Activity Assessment of Two Novel Binuclear Platinum (II) Complexes. *J. Photochem. Photobiol. B* **2016**, *161*, 345–354. DOI: 10.1016/j.jphotobiol.2016.05.025.

[5] Stevens, S. K.; Strehle, A. P.; Miller, R. L.; Gammons, S. H.; Hoffman, K. J.; McCarty, J. T.; Miller, M. E.; Stultz, L. K.; Hanson, P. K. The Anticancer Ruthenium Complex KP1019 Induces DNA Damage, Leading to Cell Cycle Delay and Cell Death in *Saccharomyces cerevisiae*. *Mol. Pharmacol.* **2013**, *83*, 225–234. DOI: 10.1124/mol.112.079657.

[6] Dragutan, I.; Dragutan, V.; Demonceau, A. Editorial of Special Issue Ruthenium Complex: The Expanding Chemistry of the Ruthenium Complexes. *Molecules* **2015**, *20*, 17244–17274. DOI: 10.3390/molecules200917244.

[7] Graf, N.; Lippard, S. J. Redox Activation of Metal-Based Prodrugs as a Strategy for Drug Delivery. *Adv. Drug Deliv. Rev.* **2012**, *64*, 993–1004. DOI: 10.1016/j.addr.2012.01.007.

[8] Lee, H. Z. S.; Buriez, O.; Labbé, E.; Top, S.; Pigeon, P.; Jaouen, G.; Amatore, C.; Leong, W. K. Oxidative Sequence of a Ruthenocene-Based Anticancer Drug Candidate in a Basic Environment. *Organometallics* **2014**, *33*, 4940–4946. DOI: 10.1021/om500225k.

[9] Furrer, J.; Süss-Fink, G. Thiolato-Bridged Dinuclear Arene Ruthenium Complexes and Their Potential as Anticancer Drugs. *Coord. Chem. Rev.* **2016**, *309*, 36–50. DOI: 10.1016/j.ccr.2015.10.007.

[10] Li, X.; Gorle, A. K.; Sundaraneedi, M. K.; Keene, F. R.; Collins, J. G. Kinetically-Inert Polypyridylruthenium(II) Complexes as Therapeutic Agents. *Coord. Chem. Rev.* **2017**, *32*, 33–47. DOI: 10.1016/j.ccr.2017.11.011.

[11] Lazarević, T.; Rilak, A.; Bugarčić, ŽD. Platinum, Palladium, Gold and Ruthenium Complexes as Anticancer Agents: Current Clinical Uses, Cytotoxicity Studies and Future Perspectives. *Eur. J. Med. Chem.* **2017**, *142*, 8–31. DOI: 10.1016/j.ejmech.2017.04.007.

[12] Wan, D.; Tang, B.; Wang, Y. J.; Guo, B. H.; Yin, H.; Yi, Q. Y.; Liu, Y. J. Synthesis and Anticancer Properties of Ruthenium (II) Complexes as Potent Apoptosis Inducers through Mitochondrial Disruption. *Eur. J. Med. Chem.* **2017**, *139*, 180–190. DOI: 10.1016/j.ejmech.2017.07.066.

[13] Michlewska, S.; Ionov, M.; Maroto-Díaz, M.; Szwed, A.; Ihnatsyeu-Kachan, A.; Loznikova, S.; Shcharbin, D.; Maly, M.; Ramirez, R. G.; de la Mata, F. J.; Bryszewska, M. Ruthenium Dendrimers as Carriers for Anticancer siRNA. *J. Inorg. Biochem.* **2018**, *181*, 18–27. DOI: 10.1016/j.jinorgbio.2018.01.001.

[14] Timerbaev, A. R. Role of Metallomic Strategies in Developing Ruthenium Anticancer Drugs. *TrAC Trends Anal. Chem.* **2016**, *80*, 547–554. DOI: 10.1016/j.trac.2016.04.015.

[15] Bergamo, A.; Sava, G. Ruthenium Anticancer Compounds: Myths and Realities of the Emerging Metal-Based Drugs. *Dalton Trans.* **2011**, *40*, 7817–7823. DOI: 10.1039/C0DT01816C.

[16] Kaulage, M. H.; Maji, B.; Pasadi, S.; Bhattacharya, S.; Muniyappa, K. Novel Ruthenium Azo-Quinoline Complexes with Enhanced Photonuclease Activity in Human Cancer Cells. *Eur. J. Med. Chem.* **2017**, *139*, 1016–1029. DOI: 10.1016/j.ejmech.2017.08.059.

[17] Sahyon, H. A.; El-Bindary, A. A.; Shoair, A. F.; Abdellatif, A. A. Synthesis and Characterization of Ruthenium(III) Complex Containing 2-Aminomethyl Benzimidazole, and Its Anticancer Activity of *In Vitro* and *In Vivo* Models. *J. Mol. Liq.* **2018**, *255*, 122–134. DOI: 10.1016/j.molliq.2018.01.140.

[18] Tikum, A. F.; Jeon, Y. J.; Lee, J. H.; Park, M. H.; Bae, I. Y.; Kim, S. H.; Lee, H. J.; Kim, J. Cytotoxic and Anticancer Properties of New Ruthenium Polypyridyl Complexes with Different Lipophilicities. *J. Inorg. Biochem.* **2018**, *180*, 204–210. DOI: 10.1016/j.jinorgbio.2018.01.003.

[19] Wei, J.; Renfrew, A. K. Photolabile Ruthenium Complexes to Cage and Release a Highly Cytotoxic Anticancer Agent. *J. Inorg. Biochem.* **2018**, *179*, 146–153. DOI: 10.1016/j.jinorgbio.2017.11.018.

[20] Tang, B.; Wan, D.; Lai, S. H.; Yang, H. H.; Zhang, C.; Wang, X. Z.; Zeng, C. C.; Liu, Y. J. Design, Synthesis and Evaluation of Anticancer Activity of Ruthenium (II) Polypyridyl Complexes. *J. Inorg. Biochem.* **2017**, *173*, 93–104. DOI: 10.1016/j.jinorgbio.2017.04.028.

[21] Dou, Y.-H.; Xu, S.-D.; Chen, Y.; Wu, X.-H. Synthesis, Characterization, and Anticancer Activity of Dithiocarbamate Ruthenium(II) Complexes. *Phosphorus Sulfur Silicon Relat. Elem.* **2017**, *192*, 1219–1223. DOI: 10.1080/10426507.2017.1359594.

[22] Ali, I.; Wani, W. A.; Saleem, K.; Hseih, M. F. Design and Synthesis of Thalidomide Based Dithiocarbamate Cu(II), Ni(II) and Ru(III) Complexes as Anticancer Agents. *Polyhedron* **2013**, *56*, 134–143. DOI: 10.1016/j.poly.2013.03.056.

[23] Scintilla, S.; Brustolin, L.; Gambalunga, A.; Chiara, F.; Trevisan, A.; Nardon, C.; Fregona, D. Ru(III) Anticancer Agents with Aromatic and Non-Aromatic Dithiocarbamates as Ligands: Loading into Nanocarriers and Preliminary Biological Studies. *J. Inorg. Biochem.* **2016**, *165*, 159–169. DOI: 10.1016/j.jinorgbio.2016.11.018.

[24] Hogarth, G. Metal-Dithiocarbamate Complexes: Chemistry and Biological Activity. *Mini Rev Med Chem* **2012**, *12*, 1202–1215. DOI: 10.2174/138955712802762095.

[25] Andrew, F. P.; Ajibade, P. A. Metal Complexes of Alkyl-Aryl Dithiocarbamates: Structural Studies, Anticancer Potentials and Applications as Precursors for Semiconductor Nanocrystals. *J. Mol. Struct.* **2018**, *1155*, 843–855. DOI: 10.1016/j.molstruc.2017.10.106.

[26] Ajibade, P. A.; Mbese, J. Z.; Omondi, B. Group 12 Dithiocarbamate Complexes: Synthesis, Characterization, and X-Ray Crystal Structures of Zn(II) and Hg(II) Complexes and Their Use as Precursors for Metal Sulphide Nanoparticles. *Inorg. Nano- Met. Chem.* **2017**, *47*, 202–212. DOI: 10.1080/15533174.2015.1137589.

[27] Mbese, J. Z.; Ajibade, P. A. Synthesis, Structural and Optical Properties of ZnS, CdS and HgS Nanoparticles from Dithiocarbamato Single Molecule Precursors. *J. Sulf. Chem.* **2014**, *35*, 438–449. DOI: 10.1080/17415993.2014.912280.

[28] Giovagnini, L.; Mancinetti, E.; Ronconi, L.; Sitran, S.; Marchiò, L.; Castagliuolo, I.; Brun, P.; Trevisan, A.; Fregona, D. Preliminary Chemico-Biological Studies on Ru(III) Compounds with *S*-Methyl Pyrrolidine/Dimethyl Dithiocarbamate. *J. Inorg. Biochem.* **2009**, *103*, 774–782. DOI: 10.1016/j.jinorgbio.2009.01.019.

[29] Khan, S. Z.; Amir, M. K.; Ullah, I.; Aamir, A.; Pezzuto, J. M.; Kondratyuk, T.; Gariepy, F. B.; Ali, A.; Khan, S. New Heteroleptic Palladium(II) Dithiocarbamates: Synthesis, Characterization, Packing and Anticancer Activity against Five Different Cancer Cell Lines. *Appl. Organomet. Chem.* **2016**, *30*, 392–398. DOI: 10.1002/aoc.3445.

[30] Bonati, F.; Ugo, R. Organotin(IV) N,N-Disubstituted Dithiocarbamates. *J. Organomet. Chem.* **1967**, *10*, 257–268. DOI: 10.1016/S0022-328X(00)93085-7.

[31] Mansouri-Torshizi, H.; Saeidifar, M.; Divsalar, A.; Saboury, A. A. Interaction Studies between a 1,10-Phenanthroline Adduct of Palladium(II) Dithiocarbamate anti-Tumor Complex and Calf Thymus DNA. A Synthesis Spectral and In-Vitro Study. *Spectrochim. Acta A Mol. Biomol. Spectrosc.* **2010**, *77*, 312–318. DOI: 10.1016/j.saa.2010.05.029.

[32] Ferreira, I. P.; de Lima, G. M.; Paniago, E. B.; Takahashi, J. A.; Pinheiro, C. B. Synthesis, Characterization and Antifungal Activity of New Dithiocarbamate-Based Complexes of Ni(II), Pd(II) and Pt(II). *Inorg. Chim. Acta* **2014**, *423*, 443–449. DOI: 10.1016/j.ica.2014.09.002.

[33] Manav, N.; Mishra, A. K.; Kaushik, N. K. In Vitro Antitumour and Antibacterial Studies of Some Pt(IV) Dithiocarbamate Complexes. *Spectrochim. Acta A Mol. Biomol. Spectrosc.* **2006**, *65*, 32–35. DOI: 10.1016/j.saa.2005.09.023.

[34] Shaheen, F.; Badshah, A.; Gielen, M.; Dusek, M.; Fejfarova, K.; de Vos, D.; Mirza, B.; B. Synthesis, Characterization, Antibacterial and Cytotoxic Activity of New Palladium(II) Complexes with Dithiocarbamate Ligands: X-Ray Structure of Bis(Dibenzyl-1-S:S0 - Dithiocarbamato)Pd(II). *J. Organomet. Chem.* **2007**, *692*, 3019–3026. DOI: 10.1016/j.jorganchem.2007.03.019.

[35] Abdullah, N. H.; Zainal, Z.; Silong, S.; Tahir, M. I. M.; Tan, K. B.; Chang, S.; K. Synthesis of Zinc Sulphide Nanoparticles from Thermal Decomposition of Zinc N-Ethyl Cyclohexyl Dithiocarbamate Complex. *Mater. Chem. Phys.* **2016**, *173*, 33–41. DOI: 10.1016/j.matchemphys.2016.01.034.

[36] Prakasam, B. A.; Lahtinen, M.; Peuronen, A.; Muruganandham, M.; Kolehmainen, E.; Haapaniemi, E.; Sillanpää, M. Synthesis, NMR Spectral and Structural Studies on Mixed Ligand Complexes of Pd(II) Dithiocarbamates: First Structural Report on Palladium(II) Dithiocarbamate with SCN^{-}Ligand. *J. Mol. Struct.* **2016**, *1108*, 195–202. DOI: 10.1016/j.molstruc.2015.11.076.

[37] Onwudiwe, D. C.; Ajibade, P. A.; Omondi, B. Synthesis, Spectral and Thermal Studies of 2,2′-Bipyridyl Adducts of Bis(N-alkyl-N-Phenyldithiocarbamato)Zinc(II). *J. Mol. Struct.* **2011**, *987*, 58–66. DOI: 10.1016/j.molstruc.2010.11.060.

[38] Govindaswamy, P.; Mozharivskyj, Y. A.; Kollipara, M. R. Synthesis and Characterization of Cyclopentadienylruthenium(II) Complexes Containing *N,N′*-Donor Schiff Base Ligands: Crystal and Molecular Structure of $[(\eta^5\text{-}C_5H_5)Ru(C_5H_4N\text{-}2\text{-}CHN\text{–}C_6H_4\text{–}p\text{-}OCH_3)(PPh_3)]PF_6$. *Polyhedron* **2004**, *23*, 1567–1572. DOI: 10.1016/j.poly.2004.03.007.

[39] Santos, K.; Dinelli, L. R.; Bogado, A. L.; Ramos, L. A.; Cavalheiro, E. T.; Ellena, J.; Castellano, E. E.; Batista, A. A. Crystal Structure and Catalytic Activity of Ruthenium (II)/Dithiocarbamate Complexes in the Epoxidation of Cyclooctene. *Inorg. Chim. Acta* **2015**, *429*, 237–242. DOI: 10.1016/j.ica.2015.02.014.

[40] Darwish, H. W.; Barakat, A.; Nafady, A.; Suleiman, M.; Al-Noaimi, M.; Hammouti, B.; Radi, S.; Hadda, T. B.; Abu-Obaid, A.; Mubarak, M. S.; Warad, I. Design, Synthesis, Characterization of Novel Ruthenium(II) Catalysts: Highly Efficient and Selective Hydrogenation of Cinnamaldehyde to (*E*)-3-Phenylprop-2-en-1-ol. *Molecules* **2014**, *19*, 5965–5980. DOI: 10.3390/molecules19055965.

[41] Kulkarni, A. D.; Patil, S. A.; Badami, P. S. Electrochemical Properties of Some Transition Metal Complexes: Synthesis, Characterization and In-Vitro Antimicrobial Studies of Co(II), Ni(II), Cu(II), Mn(II) and Fe(III) Complexes. *Int. J. Electrochem. Sci.* **2009**, *4*, 717–729.

[42] Botha, N. L.; Ajibade, P. A. Effect of Temperature on Crystallite Sizes of Copper Sulfide Nanocrystals Prepared from Copper(II) Dithiocarbamate Single Source Precursor. *Mater. Sci. Semicon. Process.* **2016**, *43*, 149–154. DOI: 10.1016/j.mssp.2015.12.006.

[43] Devagi, G.; Dallemer, F.; Kalaivani, P.; Prabhakaran, R. Organometallic Ruthenium(II) Complexes Containing NS Donor Schiff Bases: Synthesis, Structure, Electrochemistry, DNA/BSA Binding, DNA Cleavage, Radical Scavenging and Antibacterial Activities. *J. Organomet. Chem.* **2018**, *854*, 1–14. DOI: 10.1016/j.jorganchem.2017.10.036.

[44] Andrew, F. P.; Ajibade, P. A. Synthesis, Characterization and Anticancer Studies of Bis- (N-Methyl-1-Phenyldithiocarbamato) Cu(II), Zn(II), and Pt(II) Complexes: Single Crystal X-Ray Structure of the Copper Complex. *J. Coord. Chem.* **2018**, *71*, 2776–2786. DOI: 10.1080/00958972.2018.1489537.

[45] Andrew, F. P.; Ajibade, P. A. Synthesis, Characterization and Anticancer Studies of Bis(1-Phenylpiperazine Dithiocarbamato) Cu(II), Zn(II) and Pt(II) Complexes: Crystal Structures of 1-Phenylpiperazine dithiocarbamato-S,S′ Zinc(II) and Pt(II). *J. Mol. Struct.* **2018**, *1170*, 24–29. DOI: 10.1016/j.molstruc.2018.05.068.

[46] Ajibade, P. A.; Andrew, F. P.; Botha, N. L.; Solomane, N. Synthesis, Crystal Structures and Anticancer Studies of Morpholinyldithiocarbamato Cu(II) and Zn(II) Complexes. *Molecules* **2020**, *25*, 3584. DOI: 10.3390/molecules25163584.

[47] Vijayan, P.; Viswanathamurthi, P.; Sugumar, P.; Ponnuswamy, M. N.; Balakumaran, M. D.; Kalaichelvan, P. T.; Velmurugan, K.; Nandhakumar, R.; Butcher, R. J. Unprecedented Formation of Organo-Ruthenium(II) Complexes Containing 2-Hydroxy-1-Naphthaldehyde *S*-Benzyldithiocarbazate: Synthesis, X-Ray Crystal Structure, DFT Study and Their Biological Activities *In Vitro*. *Inorg. Chem. Front.* **2015**, *2*, 620–639. DOI: 10.1039/C5QI00029G.

[48] Ramesh, R.; Sivagamasundari, M. Synthesis, Spectral and Antifungal Activity of Ru(II) Mixed-Ligand Complexes. *Synth. React. Inorg. Met.* **2003**, *33*, 899–910. DOI: 10.1081/SIM-120021656.